

Cyclic Peptoids

Sung Bin Y. Shin,[†] Barney Yoo,[†] Louis J. Todaro,[‡] and Kent Kirshenbaum^{*†}

Contribution from the Department of Chemistry, New York University, 100 Washington Square East, New York, New York 10003-6688, and Department of Chemistry, Hunter College of the City University of New York, 695 Park Avenue, New York, New York 10021

Received October 2, 2006; E-mail: kent@nyu.edu

Abstract: Foldamers are an intriguing family of biomimetic oligomers that exhibit a propensity to adopt stable secondary structures. *N*-Substituted glycine oligomers, or “peptoids”, are a prototypical example of these foldamer systems and are known to form a helix resembling that of polyproline type I. Ongoing studies seek to improve the stability of peptoid folding and to discover new secondary structure motifs. Here, we report that peptoids undergo highly efficient head-to-tail macrocyclization reactions. A diverse array of peptoid sequences from pentamers to 20mers were converted to macrocyclic products within 5 min at room temperature. The introduction of the covalent constraint enhances conformational ordering, allowing for the crystallization of a cyclic peptoid hexamer and octamer. We present the first X-ray crystallographic structures of peptoid hetero-oligomers, revealing that peptoid macrocycles can form a reverse-turn conformation.

Introduction

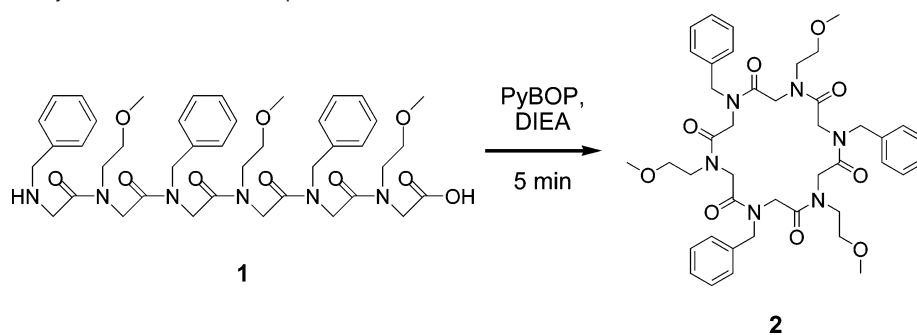
Conformational ordering is a typical characteristic of biologically active oligomers. The spatially defined presentation of pharmacophoric groups in natural and synthetic compounds can provide enhanced binding affinities, which is often attributed to diminished entropic penalties for complex formation. For example, bioactive peptides isolated from living systems are commonly found to include macrocyclic constraints that rigidify these structures.¹ Over the course of several decades, chemists have established a variety of methods to form cyclic peptides from synthetic linear precursors.^{1–4} Extensive efforts have similarly been devoted to the synthesis of peptidomimetic oligomers.^{3,5} These molecules can be designed to display chemical moieties analogous to the bioactive peptide side chains that provide critical intermolecular contacts. The abiotic character of the peptidomimetic scaffold is of potential pharmacological benefit, as it can confer protection from proteolytic

degradation. Recent studies have led to the discovery of a family of peptidomimetic oligomers that have a strong propensity to adopt stable secondary structures.⁶ The conformational ordering of these “foldamers” suggests that they may be well suited for addressing biomedical applications, including antagonizing protein–protein interactions.^{5,7} Additional studies are required to establish general design principles that enforce the stable and predictable folding of abiotic oligomer sequences.⁶

Our investigations are focused on a class of peptidomimetics called peptoids.⁸ These foldamers can be efficiently synthesized to incorporate specific sequences of chemically diverse *N*-substituted glycine monomer units.⁹ Peptoids are broadly resistant to proteolytic degradation and a variety of bioactive

[†] New York University.[‡] Hunter College of the City University of New York.

- (1) (a) Sewald, N.; Jakubke, D. H. *Peptides: Chemistry and Biology*; Wiley-VCH: Weinheim, Germany: 2002; (b) Wipf, P. *Chem. Rev.* **1995**, *95*, 2115–2134.
- (2) (a) Fasan, R.; Dias, R. L. A.; Moehle, K.; Zerbe, O.; Vrijbloed, J. W.; Obrecht, D.; Robinson, J. A. *Angew. Chem., Int. Ed.* **2004**, *43*, 2109–2112. (b) Wang, D. Y.; Liao, W.; Arora, P. S. *Angew. Chem., Int. Ed.* **2005**, *44*, 6525–6529. (c) Rizo, J.; Gierasch, L. M. *Annu. Rev. Biochem.* **1992**, *61*, 387–418. (d) Blankenstein, J.; Zhu, J. P. *Eur. J. Org. Chem.* **2005**, 1949–1964. (e) Schafmeister, C. E.; Po, J.; Verdine, G. L. *J. Am. Chem. Soc.* **2000**, *122*, 5891–5892. (f) Davies, J. S. *J. Pept. Sci.* **2003**, *9*, 471–501. (g) Hartgerink, J. D.; Granja, J. R.; Milligan, R. A.; Ghadiri, M. R. *J. Am. Chem. Soc.* **1996**, *118*, 43–50. (h) Horton, D. A.; Bourne, G. T.; Smythe, M. L. *Mol. Div.* **2000**, *5*, 289–304.
- (3) (a) Fairlie, D. P.; Abbenante, G.; March, D. R. *Curr. Med. Chem.* **1995**, *2*, 654–686. (b) Li, P.; Roller, P. P.; Xu, J. C. *Curr. Org. Chem.* **2002**, *6*, 411–440. (c) Barrett, A. G.; Hennessy, A. J.; Le, Vezouet, R.; Procopiou, P. A.; Seale, P. W.; Stefaniak, S.; Upton, R. J.; White, A. J.; Williams, D. J. *J. Org. Chem.* **2004**, *69*, 1028–37. (d) Becerril, J.; Bolte, M.; Burguete, M. I.; Galindo, F.; Garcia-Espana, E.; Luis, S. V.; Miravet, J. F. *J. Am. Chem. Soc.* **2003**, *125*, 6677–6686. (e) Dale, J.; Titlesta, K. *J. Chem. Soc., Chem. Commun.* **1969**, 656–659.
- (4) Che, Y.; Marshall, G. R. *J. Med. Chem.* **2006**, *49*, 111–124.
- (5) (a) Gademann, K.; Ernst, M.; Hoyer, D.; Seebach, D. *Angew. Chem., Int. Ed.* **1999**, *38*, 1223–1226. (b) Robinson, J. A.; Shankaramma, S. C.; Jettera, P.; Kienzl, U.; Schwendener, R. A.; Vrijbloed, J. W.; Obrecht, D. *Bioorg. Med. Chem.* **2005**, *13*, 2055–2064. (c) Wels, B.; Kruijtzter, J. A. W.; Garner, K. M.; Adan, R. A. H.; Liskamp, R. M. J. *Bioorg. Med. Chem. Lett.* **2005**, *15*, 287–290. (d) Shankaramma, S. C.; Moehle, K.; James, S.; Vrijbloed, J. W.; Obrecht, D.; Robinson, J. A. *Chem. Commun.* **2003**, 1842–1843. (e) Locardi, E.; Stockle, M.; Gruner, S.; Kessler, H. *J. Am. Chem. Soc.* **2001**, *123*, 8189–8196. (f) Chakraborty, T. K.; Srinivasu, P.; Bikshapathy, E.; Nagaraj, R.; Vairamani, M.; Kumar, S. K.; Kunwar, A. C. *J. Org. Chem.* **2003**, *68*, 6257–6263. (g) Angell, Y.; Burgess, K. *J. Org. Chem.* **2005**, *70*, 9595–9598. (h) Norgren, A. S.; Buttner, F.; Prabpai, S.; Kongsaree, P.; Arvidsson, P. I. *J. Org. Chem.* **2006**, *71*, 6814–6821. (i) Clark, T. D.; Buehler, L. K.; Ghadiri, M. R. *J. Am. Chem. Soc.* **1998**, *120*, 651–656. (j) Yuan, L. H.; Feng, W.; Yamato, K.; Sanford, A. R.; Xu, D. G.; Guo, H.; Gong, B. *J. Am. Chem. Soc.* **2004**, *126*, 11120–11121. (k) Nnanabu, E.; Burgess, K. *Org. Lett.* **2006**, *8*, 1259–62. (l) Jiang, H.; Leger, J. M.; Guionneau, P.; Huc, I. *Org. Lett.* **2004**, *6*, 2985–2988. (m) Mann, E.; Kessler, H. *Org. Lett.* **2003**, *5*, 4567–4570. (n) Wels, B.; Kruijtzter, J. A. W.; Liskamp, R. M. J. *Org. Lett.* **2002**, *4*, 2173–2176. (o) Bru, M.; Alfonso, I.; Burguete, M. I.; Luis, S. V. *Tetrahedron Lett.* **2005**, *46*, 7781–7785. (p) Vaz, E.; Brunsveld, L. *Org. Lett.* **2006**, *8*, 4199–4202. (q) Buttner, F.; Norgren, A. S.; Zhang, S. D.; Prabpai, S.; Kongsaree, P.; Arvidsson, P. I. *Chem.–Eur. J.* **2005**, *11*, 6145–6158. (r) Royo, M.; Farrera-Sinfreu, J.; Sole, L.; Albericio, F. *Tetrahedron Lett.* **2002**, *43*, 2029–2032.
- (6) (a) Gellman, S. H. *Acc. Chem. Res.* **1998**, *31*, 173–180. (b) Hill, D. J.; Mio, M. J.; Prince, R. B.; Hughes, T. S.; Moore, J. S. *Chem. Rev.* **2001**, *101*, 3893–4011. (c) Seebach, D.; Beck, A. K.; Bierbaum, D. *J. Chem. Biodiv.* **2004**, *1*, 1111–1239. (d) Cheng, R. P. *Curr. Opin. Struct. Biol.* **2004**, *14*, 512–520.

Scheme 1. Head-to-Tail Cyclization of a Linear Peptoid Hexamer

peptoid compounds have been reported.¹⁰ Peptoid sequences comprised of bulky chiral side chains have the capacity to adopt a stable helical secondary structure, although some conformational heterogeneity is evident in solution.¹¹ The crystal structure of a linear peptoid homopentamer composed of bulky chiral side chains exhibited a helical conformation resembling that of a polyproline type I helix.^{11c} More recently, NMR studies were used to elucidate the conformation of a linear peptoid homooligomer composed of chiral aromatic side chains.^{11d} This structure exhibited an irregular “threaded loop” conformation comprised of four *cis* and four *trans* amide bonds. Interestingly, this threaded loop was stabilized by intramolecular hydrogen bonding between the N- and C-termini in aprotic solvents.

We seek to expand the diversity of structural motifs accessible to peptoids as part of the broader effort to discover new functional capabilities for foldamers.¹² The introduction of covalent constraints is one approach that may aid in the design of novel peptoid motifs. In addition, such constraints may further rigidify peptoid structure, potentially augmenting the ability of

peptoid sequences for selective molecular recognition. This study reports that peptoids undergo very efficient head-to-tail cyclization using standard coupling chemistries. The introduction of the covalent constraint enforces conformational ordering, thus facilitating the crystallization of a cyclic peptoid hexamer and octamer. We report herein the first X-ray crystallographic structures of peptoid hetero-oligomers and observe that peptoids possess the capacity to form reverse-turn type secondary structures.

Results and Discussion

Cyclization of Linear Hetero-oligomers. Peptoid hexamer **1**, incorporating methoxyethyl and phenylmethyl side chains, was synthesized on 2-chlorotrityl resin, using peptoid “sub-monomer” protocols.⁹ To effect head-to-tail cyclization of the linear peptoid C-terminal acid, preliminary studies were conducted in which several acylating agents were evaluated: PyBOP, PyBrOP, HCTU, and DIC (Supporting Information). All agents successfully generated the desired cyclic hexamer in good yield, as determined by reversed-phase high-pressure liquid chromatography (RP-HPLC). PyBrOP, however, exhibited markedly lower yields with significant levels of side products. PyBOP was selected for further examination and optimization. Cyclization of **1** in the presence of PyBOP proved to be remarkably efficient (Scheme 1). Within 5 min at room temperature, the linear hexamer was converted to cyclic product **2**, with a yield of 97% as determined by HPLC (Figure 1). Low levels of intermolecular ligation products were detected (<1%). High-resolution electrospray ionization mass spectrometry (ESI-MS) confirmed a mass decrease of 18 amu, corresponding to a loss of H₂O, consistent with intramolecular condensation ($[M + H]^+$ for **2**, calcd *m/z*: 787.3952; obsd *m/z*: 787.4011).

To determine optimal chain lengths for head-to-tail cyclization, linear peptoids of various sizes (compounds **3–8**) incorporating alternating methoxyethyl and phenylmethyl residues were converted to macrocyclic peptoids (compounds **9–14**, Scheme 2 and Table 1). Cyclization of oligomers shorter than hexamer chain lengths was anticipated to proceed with poor yields, as difficulties associated with the cyclization of tetramer and pentamer peptides due to ring strain have been previously reported.^{2f,3e,13} Consistent with such studies, the cyclization of linear tetramer **3** proved challenging. Conversion of **3** into **9** exhibited only 12% yield within 5 min. The major product of this reaction was the cyclohomodimer **11**. However, pentamer **4** produced the desired macrocycle **10** in high yields (89%).

Linear octamer and decamer peptoids (compounds **5** and **6**, respectively) underwent conversion to cyclic compounds **11** and

- (7) (a) Yin, H.; Hamilton, A. D. *Angew. Chem., Int. Ed.* **2005**, *44*, 4130–63. (b) Kritzer, J. A.; Lear, J. D.; Hodsdon, M. E.; Schepartz, A. *J. Am. Chem. Soc.* **2004**, *126*, 9468–9469. (c) Yin, H.; Lee, G. I.; Sedey, K. A.; Kutzki, O.; Park, H. S.; Orner, B. P.; Ernst, J. T.; Wang, H. G.; Sebtü, S. M.; Hamilton, A. D. *J. Am. Chem. Soc.* **2005**, *127*, 10191–10196. (d) Sadowsky, J. D.; Schmitt, M. A.; Lee, H. S.; Umezawa, N.; Wang, S. M.; Tomita, Y.; Gellman, S. H. *J. Am. Chem. Soc.* **2005**, *127*, 11966–11968. (e) Stephens, O. M.; Kim, S.; Welch, B. D.; Hodsdon, M. E.; Kay, M. S.; Schepartz, A. *J. Am. Chem. Soc.* **2005**, *127*, 13126–13127. (f) Hara, T.; Durell, S. R.; Myers, M. C.; Appella, D. H. *J. Am. Chem. Soc.* **2006**, *128*, 1995–2004.
- (8) Patch, J. A.; Kirshenbaum, K.; Seuryneck, S. L.; Zuckermann, R. N. In *Pseudo-peptides in Drug Development*; Nielson, P. E., Ed.; Wiley-VCH: Weinheim, Germany, 2004; pp 1–35.
- (9) (a) Figliozzi, G. M.; Goldsmith, R.; Ng, S. C.; Banville, S. C.; Zuckermann, R. N.; John, N. A. Synthesis of N-substituted glycine peptoid libraries. In *Methods in Enzymology*; Academic Press: 1996; Vol. 267, pp 437–447. (b) Bartlett, P. A., et al. *Proc. Natl. Acad. Sci. U.S.A.* **1992**, *89*, 9367–9371.
- (10) (a) Miller, S. M.; Simon, R. J.; Ng, S.; Zuckermann, R. N.; Kerr, J. M.; Moos, W. H. *Drug Dev. Res.* **1995**, *35*, 20–32. (b) Murphy, J. E.; Uno, T.; Hamer, J. D.; Cohen, F. E.; Dworki, V.; Zuckermann, R. N. *Proc. Natl. Acad. Sci. U.S.A.* **1998**, *95*, 1517–1522. (c) Nguyen, J. T.; Turck, C. W.; Cohen, F. E.; Zuckermann, R. N.; Lim, W. A. *Science* **1998**, *282*, 2088–2092. (d) Patch, J. A.; Barron, A. E. *J. Am. Chem. Soc.* **2003**, *125*, 12092–12093. (e) Wender, P. A.; Mitchell, D. J.; Pattabiraman, K.; Pelkey, E. T.; Steinman, L.; Rothbard, J. B. *Proc. Natl. Acad. Sci. U.S.A.* **2000**, *97*, 13003–13008. (f) Wu, C. W.; Seuryneck, S. L.; Lee, K. Y. C.; Barron, A. E. *Chem. Biol.* **2003**, *10*, 1057–1063.
- (11) (a) Armand, P.; Kirshenbaum, K.; Goldsmith, R. A.; Farr-Jones, S.; Barron, A. E.; Truong, K. T. V.; Dill, K. A.; Mierke, D. F.; Cohen, F. E.; Zuckermann, R. N.; Bradley, E. K. *Proc. Natl. Acad. Sci. U.S.A.* **1998**, *95*, 4309–4314. (b) Kirshenbaum, K.; Barron, A. E.; Goldsmith, R. A.; Armand, P.; Bradley, E. K.; Truong, K. T. V.; Dill, K. A.; Cohen, F. E.; Zuckermann, R. N. *Proc. Natl. Acad. Sci. U.S.A.* **1998**, *95*, 4303–4308. (c) Wu, C. W.; Kirshenbaum, K.; Sanborn, T. J.; Patch, J. A.; Huang, K.; Dill, K. A.; Zuckermann, R. N.; Barron, A. E. *J. Am. Chem. Soc.* **2003**, *125*, 13525–13530. (d) Huang, K.; Wu, C. W.; Sanborn, T. J.; Patch, J. A.; Kirshenbaum, K.; Zuckermann, R. N.; Barron, A. E.; Radhakrishnan, I. *J. Am. Chem. Soc.* **2006**, *128*, 1733–1738. (e) Lee, Y. C.; Zuckermann, R. N.; Dill, K. A. *J. Am. Chem. Soc.* **2005**, *127*, 10999–11009.
- (12) Jang, H. J.; Fafarman, A.; Holub, J. M.; Kirshenbaum, K. *Org. Lett.* **2005**, *7*, 1951–1954.

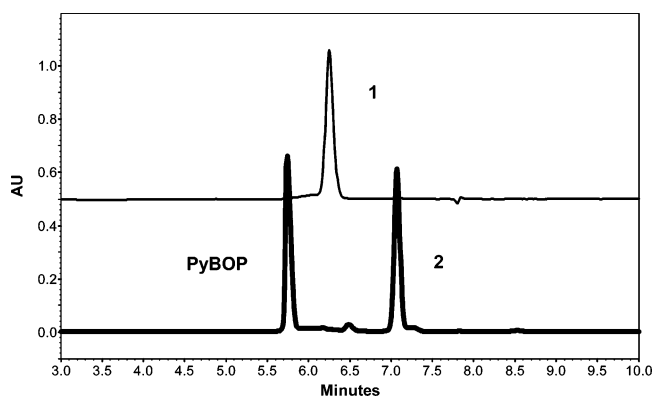


Figure 1. Rapid macrocyclization of peptoid hexamer **1**. Analytical RP-HPLC (214 nm) of reaction described in Scheme 1. Upper trace (offset in y-direction) shows reaction prior to addition of PyBOP acylating agent. Lower trace is reaction 5 min after PyBOP addition.

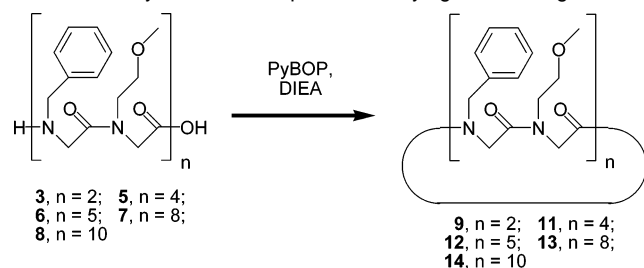
Table 1. Macrocyclization of Linear Peptoid Oligomers

compound no.		chain length	linear sequence ^b	yield ^c (%)
linear	cyclic ^a			
1	2	6	(Npm-Nme) ₃	97
3	9	4	(Npm-Nme) ₂	12
4	10	5	Npm-Nme-Npm-Nme-Npm	89
5	11	8	(Npm-Nme) ₄	93
6	12	10	(Npm-Nme) ₅	97
7	13	16	(Npm-Nme) ₈	95
8	14	20	(Npm-Nme) ₁₀	91
15	16	6	(Naz-Nme) ₃	87
17	18	12	(Naz-Nme-Npm) ₄	75
19	20	6	(Ncb-Nme) ₃	71
21	22	10	Npc-Ntp-Nip-Npc-Nib-Nip-Nib-Npm-Npm-Ntp	87
23	24	6	(Hse ^(Me) -Phe) ₃	39

^a Product from linear oligomer; cyclization conditions described in text.

^b Side chain abbreviations are in Experimental Procedures. Compound **23** is the peptide analog of peptoid **1**. ^c Yields of cyclic product as determined by RP-HPLC.

Scheme 2. Cyclization of Peptoids of Varying Chain Lengths



12 with high yields, similar to that observed for the hexamer (Table 1). Remarkably, 16mer and 20mer peptoids (compounds **7** and **8**, respectively) also formed the 48-atom and 60-atom macrocyclic products **13** and **14** rapidly and in high yields.

Efficient macrocyclization of peptoids was observed for sequences that contain diverse chemical functionalities. A hexamer sequence **15** with alternating methoxyethyl and azidopropyl side chains was cyclized, resulting in efficient

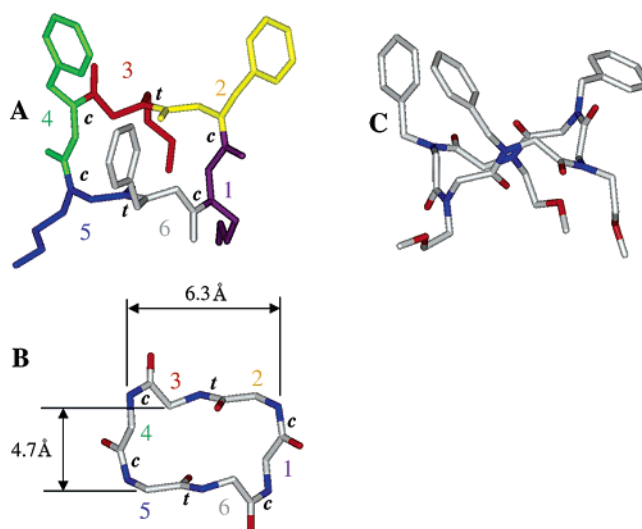


Figure 2. Crystal structure of cyclic peptoid hexamer **2** showing segregation of polar and apolar side chains on opposing faces of the macrocycle. (A) Top view. Purple – residue 1, yellow – residue 2, red – residue 3, green – residue 4, blue – residue 5, gray – residue 6, c – cis, t – trans; (B) Top view backbone; (C) Side view.

formation of product **16** (87%). A dodecamer sequence **17**, containing azidopropyl, phenylmethyl, and methoxyethyl residues, was also cyclized with good yields (macrocycle **18**, 75%). A hexamer sequence **19** incorporating Boc (*tert*-butoxycarbonyl) protected aminobutyl groups was cyclized to form the product **20** (71%). In addition, a highly chemically diverse decamer sequence **21**, the peptoid analogue of the α -amino acid peptide Orn^(Boc)-Asp^(*tert*-butyl)-Val-Orn^(Boc)-Leu-Val-Leu-Phe-Phe-Asp^(*tert*-butyl), was cyclized to form **22** (87%).

Whereas the above reactions were conducted at moderately dilute concentrations of the linear oligomer starting materials (1.7 mg/mL; 0.6–3.0 mM), we evaluated the possibility of conducting these reactions at higher concentrations. Compound **5** was subjected to cyclization reactions following the previously described protocols. We observed the rapid formation of the desired macrocycles without significant accumulation of intermolecular reaction products at concentrations ranging from 0.3 to 78 mM.

All reactions described above were completed at room temperature for 5 min, suggesting that peptoids may possess properties that facilitate rapid macrocyclization. The efficiency of the cyclization reaction of **1** was compared with its corresponding α -amino acid sequence **23**. Conversion of **23** into **24** showed only a 39% yield under the same conditions (whereas the yield of **1** to form macrocycle **2** was 97%). Several studies in model peptide sequences have shown that incorporation of *N*-alkylated amino acid residues can assist intramolecular cyclization.^{2d,2f,3e} By reducing the energy barrier for interconversion between amide *cisoid* and *transoid* forms, such sequences may be prone to adopt turn structures, facilitating cyclization of linear peptides.¹⁴ Peptoids are composed of *N*-substituted glycine units, and linear peptoid oligomers have been shown to readily undergo *cis/trans* isomerization. Therefore, peptoids may be capable of efficiently sampling greater conformational space than corresponding peptide sequences,⁸ allowing peptoids to readily populate states favorable for

(13) (a) Meutermans, W. D. F.; Bourne, G. T.; Golding, S. W.; Horton, D. A.; Campitelli, M. R.; Craik, D.; Scanlon, M.; Smythe, M. L. *Org. Lett.* **2003**, *5*, 2711–2714. (b) Cavellierfrontin, F.; Achmad, S.; Verducci, J.; Jacquier, R.; Pepe, G. *THEOCHEM* **1993**, *105*, 125–130. (c) Mästle, W.; Link, U.; Witschel, W.; Thewalt, U.; Weber, T.; Rothe, M. *Biopolymers* **1991**, *31*, 735–744. (d) Ehrlich, A.; Heyne, H. U.; Winter, R.; Beyersmann, M.; Haber, H.; Carpino, L. A.; Bienert, M. *J. Org. Chem.* **1996**, *61*, 8831–8838. (e) Schmidt, U.; Langner, J. *J. Pept. Res.* **1997**, *49*, 67–73. (f) Nishino, N.; Xu, M.; Mihara, H.; Fujimoto, T.; Ueno, Y.; Kumagai, H. *Tetrahedron Lett.* **1992**, *33*, 1479–1482.

(14) Scherer, G.; Kramer, M. L.; Schutkowski, M.; Reimer, U.; Fischer, G. *J. Am. Chem. Soc.* **1998**, *120*, 5568–5574.

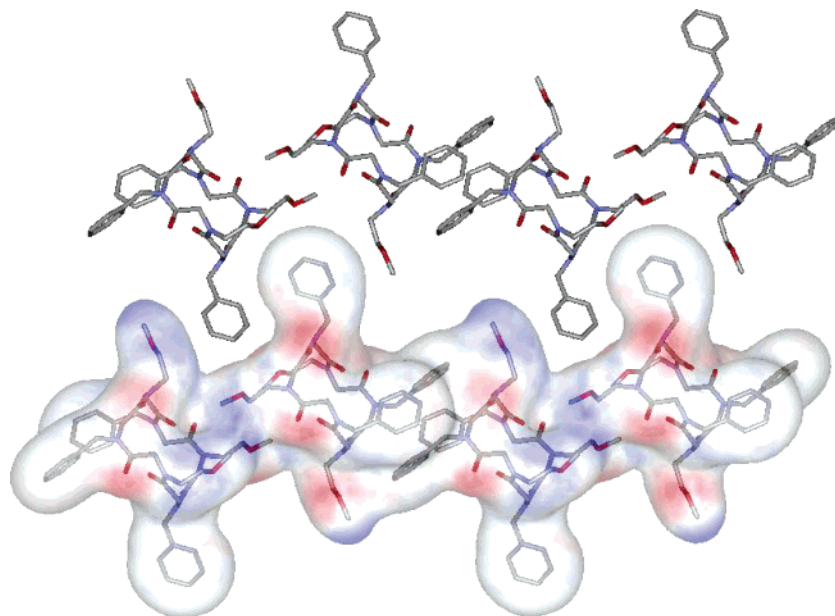


Figure 3. Crystal structure of cyclic peptoid hexamer **2**. Four unit cells are shown.

condensation of the N- and C-termini. In addition, macrocyclization may be further enhanced by the presence of a terminal secondary amine, as these groups are known to be more nucleophilic than corresponding primary amines with similar pK_a 's, and thus can exhibit greater reactivity.¹⁵

Structure of Cyclic Peptoid Hexamer. Cyclic hexamer **2** was observed to readily form needlelike crystals overnight from an NMR sample prepared in methanol- d_4 . A more controlled crystallization of **2** was then performed by slow evaporation of solutions in methanol. X-ray crystallographic studies were used to elucidate the high-resolution structure of **2** (Figure 2). The unit cell of the crystal consists of two stacked peptoid molecules in which the contact surface is comprised of four methoxyethyl groups. For each molecule, the more hydrophilic methoxyethyl side groups are segregated to one face of the macrocycle and the apolar hydrophobic phenyl groups are situated on the opposing face. The peptoid backbone of **2** takes on an overall rectangular form, with dimensions of approximately 4.7 Å by 6.3 Å. Four *cis* amide bonds reside at each corner, with two *trans* amide bonds present on two opposing sides (Figure 2).

The phenyl groups provide both intramolecular aromatic contacts (phenyl centroid-to-centroid distance, 5.73 Å) as well as intermolecular aromatic contacts between unit cells (phenyl centroid-to-centroid distance, 5.15 Å). The clustering of phenyl-phenyl moieties may help to both direct the conformation of each hexamer and also specify crystal packing geometry.¹⁶ Protruding phenyl and methoxyethyl side chains enable lateral packing by creating a cavity into which a second set of side chains from neighboring unit cells can interdigitate (Figure 3).

Structure of a Cyclic Peptoid Octamer. Crystals of cyclic octamer **11** were obtained by slow evaporation in ethanol, and a high-resolution structure was obtained by X-ray diffraction studies (Figure 4). The unit cell of the crystal is composed of four macrocycles with two distinct conformations. Although the

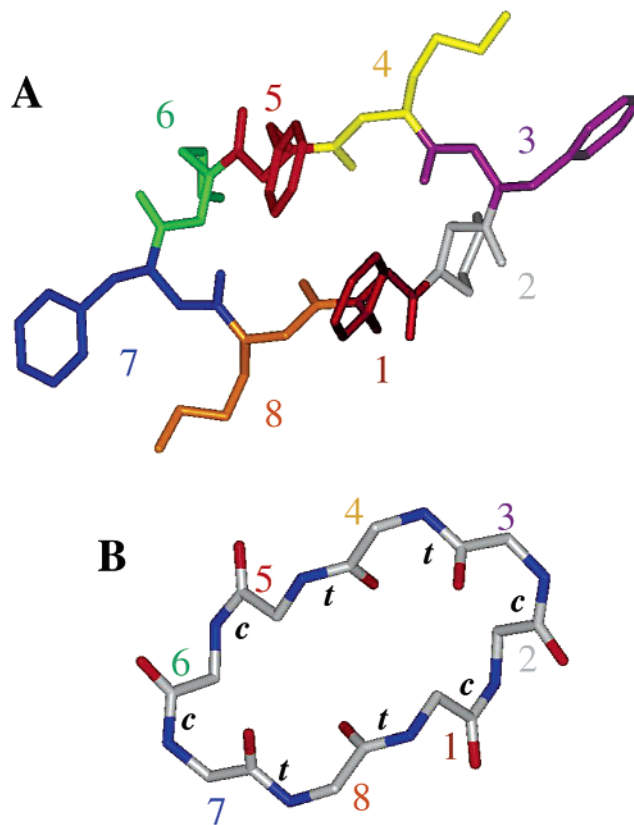


Figure 4. X-ray crystal structure of peptoid octamer **11**. (A) Top view. Brown – residue 1, gray – residue 2, purple – residue 3, yellow – residue 4, red – residue 5, green – residue 6, blue – residue 7, orange – residue 8; (B) Backbone. *c* – *cis*, *t* – *trans*. Overall dimensions are 4.8 Å by 8.0 Å.

overall geometries of the backbones are similar, variations in the χ_2 dihedral angles of the phenylmethyl side chains are observed. As observed in hexamer **2**, the backbone of **11** assumes a compact rectangular form with dimensions approximately 4.8 Å by 8.0 Å. Four *cis* and four *trans* amide bonds are present and alternate in pairs (Figure 4b).

The side chains of each macrocycle are presented in alternating lateral and axial orientations. Two axial phenylmethyl side

(15) (a) Bunting, J. W.; Mason, J. M.; Heo, C. K. M. *J. Chem. Soc., Perkin Trans. 2* **1994**, 2291–2300. (b) Buncel, E.; Um, I. H. *Tetrahedron* **2004**, *60*, 7801–7825.

(16) Bong, D. T.; Ghadiri, M. R. *Angew. Chem., Int. Ed.* **2001**, *40*, 2163–2166.

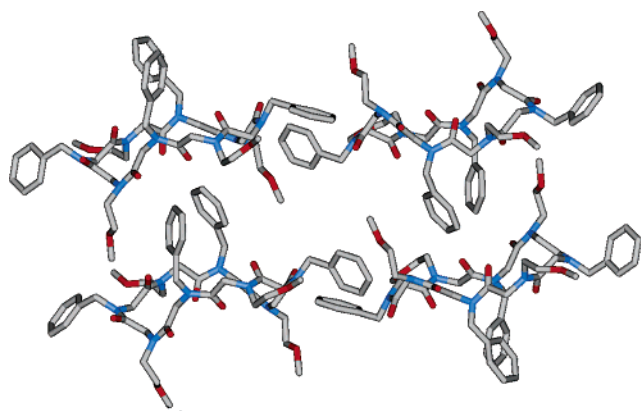


Figure 5. X-ray crystal structure of octamer **11**. Side view of one unit cell including four molecules is shown.

Table 2. Dihedral Angles and Distortion Parameters of Compound **2**

residues	φ	ψ	χ_1	ω	τ^a	χ_C^b	χ_N^c
1	-78.5°	137.9°	-85.7°	-15.0°	-15.1° (15.1)	6.1°	6.2°
2	80.4°	-172.1°	89.8°	8.5°	2.7° (2.7)	-1.4°	10.2°
3	71.5°	-170.8°	127.0°	163.4°	171.8° (8.2)	2.9°	-13.8°
4	90.9°	149.3°	95.9°	15.9°	12.5° (12.5)	-6.0°	0.9°
5	-76.6°	164.5°	-82.3°	-4.5°	1.0° (1.0)	0.4°	-10.6°
6	-81.2°	170.5°	-101.5°	-169.0°	-175.2° (4.8)	-1.5°	10.8°

^a $\tau = (\omega_1 + \omega_2)/2$; value in parentheses corresponds to deviations from planarity. ^b $\chi_C = \omega_1 - \omega_3 + \pi$. ^c $\chi_N = \omega_2 - \omega_3 + \pi$.^{17b,c}

Table 3. Dihedral Angles and Distortion Parameters of the Two Conformers Observed in the Unit Cell of Compound **11**

residues	φ	ψ	χ_1	ω	τ^a	χ_C^b	χ_N^c
1	-75.1°	170.9°	-105.5°	-178.3°	-176.5° (3.5)	1.9°	5.6°
2	-93.1°	175.5°	-84.6°	15.7°	4.5° (4.5)	1.0°	-21.4°
3	76.3°	179.3°	125.1°	18.5°	7.5° (7.5)	3.5°	-18.6°
4	72.0°	178.7°	128.0°	164.8°	-185.6° (5.6)	-1.0°	18.3°
5	-73.6°	-172.1°	-96.6°	-177.3°	-178.7° (1.3)	1.2°	-1.6°
6	-100.4°	-176.8°	-78.2°	7.5°	2.8° (2.8)	0.3°	-9.1°
7	89.9°	-178.8°	95.4°	17.8°	5.5° (5.5)	3.7°	-20.9°
8	73.6°	173.4°	127.5°	166.1°	-183.5° (3.5)	-0.1°	20.7°
1'	69.3°	-169.9°	108.4°	-164.1°	-175.1° (4.9)	0.5°	-21.4°
2'	84.2°	-179.5°	80.4°	-7.1°	2.4° (2.4)	-14.5°	4.4°
3'	-84.3°	-175.6°	-111.5°	-20.3°	-9.1° (9.1)	-3.9°	18.6°
4'	-71.5°	-178.8°	-128.6°	-173.1°	-180.0° (0.0)	0.0°	-13.8°
5'	68.9°	-168.0°	101.3°	-167.5°	-177.5° (2.5)	0.3°	-19.7°
6'	87.5°	178.4°	81.2°	1.2°	4.4° (4.4)	1.3°	7.7°
7'	-97.3°	-176.4°	-104.4°	-18.2°	-3.8° (3.8)	-3.1°	25.7°
8'	-70.9°	-173.1°	-135.1°	-172.9°	-181.1° (1.1)	1.3°	-17.6°

^a $\tau = (\omega_1 + \omega_2)/2$; value in parentheses corresponds to deviations from planarity. ^b $\chi_C = \omega_1 - \omega_3 + \pi$. ^c $\chi_N = \omega_2 - \omega_3 + \pi$.^{17b,c}

chains from residues 1 and 5 occupy the same face of the macrocycle and form intermolecular aromatic contacts (phenyl centroid-to-centroid distances of 4.49 Å and 5.26 Å). On the opposite face, two axial methoxyethyl groups from residues 2 and 6 create a cavity into which two phenyl rings from the neighboring molecules interdigitate. The remaining four side chains assume lateral placements and promote intermolecular phenyl–phenyl interactions (Figure 5).

Backbone Dihedral Angles - Distortion of Amide Bonds.

The crystal structures show little variation in backbone φ and ψ dihedral angles for both cyclohexamer and cyclooctamer. The φ dihedral angles exhibit values near $\pm 80^\circ$, with ψ dihedral angles clustering near 180° (Tables 2 and 3). The ω dihedral angles, however, display noticeable variations. Both *cis* and *trans* conformations are observed, as well as significant deviations

of the amide bonds from planarity. The *cis* amide ω dihedral angles for the cyclic peptoids range from -20° to 18° with a mean of 1.7° and standard deviation of 14.4° . The *trans* conformer values range from 163° to 195° (equivalent to -165°) with a mean of 180.6° and a standard deviation of 12.1° .

Examinations of nonplanar amide bonds in polypeptide crystal structures have been reported.¹⁷ Analysis of cyclic peptides containing six or more residues revealed that *trans* ω dihedral angles exhibit a mean value of 179.7° and standard deviation of 5.9° . *Cis* conformations have a mean ω value of 0.5° and standard deviation of 10.9° . Thus, cyclic peptoids **2** and **11** exhibit larger standard deviations of ω dihedral values than their peptide counterparts. The *trans* ω angle standard deviation for these cyclic peptoids (14.4°) is more than twice the reported value for cyclic peptides, suggesting that cyclic peptoids may exhibit diminished strain energies for accommodating distortions of amide bonds from planarity.

The extent of distortion about the backbone amide bonds present in **2** and **11** was further analyzed using the out-of-plane bending parameters, χ_N and χ_C , and the twisting parameter, τ , as described by Winkler and Dunitz.¹⁷ The χ_N and χ_C values describe the nonplanarity about the amide bond and represent the degree of pyramidalization of the amide nitrogen and the carbonyl carbon, respectively. The τ values describe the magnitude of rotation or twist about the carbonyl carbon and the amide nitrogen. Unlike planar amide bonds, where both χ_N and χ_C values are zero, the measured χ_N values for **2** range from 0.9° to 13.8° and, for **11**, range from 1.6° to 20.9° . In particular, four of the six amide bonds in **2** possess χ_N values greater than 10° , and five of eight amide bonds in **11** possess χ_N values greater than 18° . This indicates that a substantial fraction of the amide nitrogen atoms exhibit significant pyramidal distortions in these two structures. The χ_C values for **2** and **11** also exhibit distortions, with values ranging from 0.4° to 6.1° and from 0.1° to 3.7° , respectively. However, **2** possesses carbonyl carbons with markedly greater pyramidalization ($\chi_C = 6.1^\circ$ and 6.0° for residues 1 and 4) than those observed for **11** ($\chi_C = 3.5^\circ$ and 3.7° for residues 3 and 7). The τ values for **2** and **11** exhibit varying degrees of amide bond twist, with values ranging from 1.0° to 15.1° and 1.3° to 7.5° relative to planarity. Overall, the amide bonds present in the solid-state structures of **2** and **11** deviate substantially from the idealized peptide bond. The distortion parameters, χ_N , χ_C , and τ from Tables 2 and 3, classify these amides as predominantly “twisted nonplanar” (Figure 6).¹⁷ Consistent with these distortions are increases in Nsp^2-Csp^2 amide bond lengths relative to the idealized ~ 1.33 Å for peptides. The C(O)–N bonds range from 1.350 Å to 1.360 Å for **2** and 1.347 Å to 1.359 Å for **11**. These values are indicative of diminished double bond character for the *N*-substituted amide groups. The steric congestion associated with the formation of the peptoid macrocycles could then be anticipated to result in substantial deviations of amide bond planarity as the energetic barrier to the amide bond rotation is mitigated.

Cyclic Peptoids Form Reverse Turns. There have been substantial efforts to develop techniques for the efficient

(17) (a) MacArthur, M. W.; Thornton, J. M. *J. Mol. Biol.* **1996**, *264*, 1180–95. (b) Winkler, F. K.; Dunitz, J. D. *J. Mol. Biol.* **1971**, *59*, 169–182. (c) Yamada, S. In *The Amide Linkage*; Greenberg, A., Breneman, C. M., Liebman, J. F., Eds. Wiley-Interscience: New York, 2000; pp 215–246.

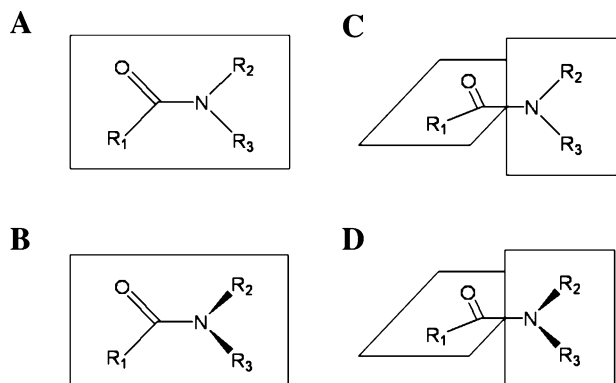


Figure 6. Amide bond types: (A) planar amide; (B) nonplanar amide; (C) twisted amide; (D) twisted nonplanar amide.^{17b,c}

synthesis of peptidomimetics capable of forming turn motifs.^{4,18} These conformations will be critical for generating synthetic mimics of biological macromolecules. Proteins, for example, utilize reverse-turn motifs to connect individual elements of secondary structure and to enable the polypeptide chain to fold into compact, globular architectures. In addition, because reverse-turns are commonly found at contact sites between proteins, turn mimetics may be capable of antagonizing critical protein–protein interactions.¹⁸ The crystal structures of cyclic hexamer **2** and octamer **11** reveal the capacity of the peptoid backbone to adopt compact conformations and accommodate tight turns. Structures **2** and **11** exhibit a pair of *cis* amide bonds at or near the corners of the rectangular backbone (residues 1/2 and 3/4 for **2**; residues 2/3 and 6/7 for **11**). These adjacent *cisoid* residues provide for a tight reversal of oligomer chain direction, with distances of ≤ 5 Å between $C\alpha_i$ and $C\alpha_i + 2$ for both macrocycles.

In proteins, the most prevalent turn motif is the β -turn, defined by a sharp 180° reversal of the protein backbone within a span of four consecutive residues, i to $i + 3$, in which the distance between $C\alpha_i$ and $C\alpha_i + 3$ is less than 7 Å and the two central residues are nonhelical.¹⁹ The tight turns formed by **2** and **11** adhere to these β -turn characteristics. The distances between $C\alpha_i$ and $C\alpha_i + 3$ are 5.0 Å for $C\alpha_3$ to $C\alpha_6$ in **2** and 5.1 Å for $C\alpha_1$ to $C\alpha_4$ in **11**. Superposition of peptoid backbone atoms (N3, $C\alpha_3$, C3, N4, $C\alpha_4$, C4, N4, $C\alpha_4$, C4, and N5) in **2** with the corresponding peptide backbone atoms ($C\alpha_i + 3$, $N_i + 3$, $C_i + 2$, $C\alpha_i + 2$, $N_i + 2$, $C_i + 1$, $C\alpha_i + 1$, $N_i + 1$, C_i , and $C\alpha_i$) of ideal β -turns (types I, I', II, II', III, III', VIa, and VIb)²⁰ reveals that the backbone conformations at the turn region of **2** closely resemble β -turn types I and III with rmsd values of 0.397

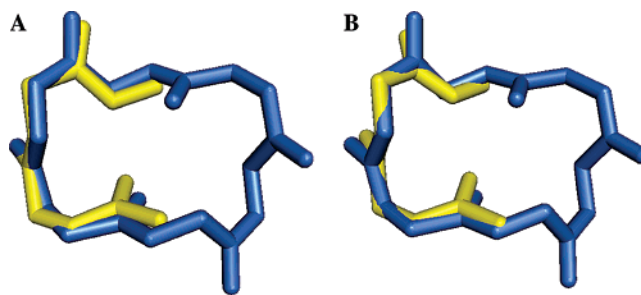


Figure 7. Superposition of the backbone atoms in cyclic peptoid hexamer **2** (blue) with canonical: (A) type I β -turn (yellow); (B) type III β -turn (yellow).

Å and 0.301 Å, respectively (Figure 7). The turn conformations of **2**, as well as **11**, demonstrate the capacity to mimic not only idealized β -turns but also the disposition of side chain groups as observed in β -turns from protein X-ray crystal structures (Figure S2b, c).

Superposition of backbone atoms at the turn regions of **2** and **11** show a high degree of similarity (rmsd: 0.318 Å for 10 atoms as listed above; Figure S2a). The overlay also demonstrates good alignment of the peptoid side chains. The structural regularity for these molecules suggests that peptoid macrocyclization may be a general platform for the development of a predictable secondary structural motif for peptoid oligomers resembling reverse-turns. The ability to incorporate a diverse array of chemical functionalities in the peptoid side chains may enable the generation of peptoid macrocycle libraries for the discovery of compounds that effectively antagonize specific protein–protein interactions.

Conclusion

We describe the efficient head-to-tail cyclization for an array of peptoid sequences and chain lengths. The conformational constraint provided by this modification enables the crystallization and X-ray structure determination of a cyclic hexamer and octamer, **2** and **11**. The high-resolution crystal structures presented here are the first reported for peptoid hetero-oligomers.

Analysis of these structures revealed the capacity for the peptoid backbone to accommodate distorted *cis* and *trans* amide conformers in the solid state. Nearly all amide bonds exhibited nonplanar twisted configurations. In addition, the capacity of the peptoid backbone to readily accommodate tight turns was noted. These results suggest head-to-tail cyclization of peptoid oligomers may provide an attractive route for the synthesis of stable mimics of peptide reverse-turn structures or enable the design of novel structural motifs not accessible to polypeptides.^{18,21}

The orientation of the side chains of peptoid **2** provides structural insights with implications for future design efforts using biomimetic oligomers. The polar and apolar side chains are segregated, accompanied by extensive nonlocal contacts of similar side chain types. This suggests it may be possible to design more complex oligomer sequences in which the patterning of side chain physicochemical properties directs the association of peptoid secondary structure elements to adopt a discrete three-dimensional structure.^{12c,22}

- (18) (a) Burgess, K. *Acc. Chem. Res.* **2001**, *34*, 826–835. (b) Souers, A. J.; Virgilio, A. A.; Schurer, S. S.; Ellman, J. A.; Kogan, T. P.; West, H. E.; Ankener, W.; Vanderslice, P. *Bioorg. Med. Chem. Lett.* **1998**, *8*, 2297–2302. (c) MacDonald, M.; Aube, J. *Curr. Org. Chem.* **2001**, *5*, 417–438. (d) Lee, H. B.; Zaccaro, M. C.; Pattarawarapan, M.; Roy, S.; Saragovi, H. U.; Burgess, K. *J. Org. Chem.* **2004**, *69*, 701–713. (e) Golebiowski, A.; Klopfenstein, S. R.; Shao, X.; Chen, J. J.; Colson, A. O.; Grieb, A. L.; Russell, A. F. *Org. Lett.* **2000**, *2*, 2615–2617. (f) Souers, A. J.; Ellman, J. A. *Tetrahedron* **2001**, *57*, 7431–7448. (g) Virgilio, A. A.; Bray, A. A.; Zhang, W.; Trinh, L.; Snyder, M.; Morrissey, M. M.; Ellman, J. A. *Tetrahedron* **1997**, *53*, 6635–6644. (h) Golebiowski, A.; Klopfenstein, S. R.; Chen, J. J.; Shao, X. *Tetrahedron Lett.* **2000**, *41*, 4841–4844. (i) Reyes, S. J.; Burgess, K. *Tetrahedron: Asymmetry* **2005**, *16*, 1061–1069. (j) Halal, L.; Lubell, W. D. *J. Org. Chem.* **1999**, *64*, 3312–3321.
- (19) Lewis, P. N.; Momany, F. A.; Scheraga, H. A. *Biochim. Biophys. Acta* **1973**, *303*, 211–229.
- (20) (a) Fink, B. E.; Kym, P. R.; Katzenellenbogen, J. A. *J. Am. Chem. Soc.* **1998**, *120*, 4334–4344. (b) Halal, L.; Lubell, W. D. *J. Am. Chem. Soc.* **2002**, *124*, 2474–2484.

- (21) Chatterjee, J.; Mierke, D.; Kessler, H. *J. Am. Chem. Soc.* **2006**, *128*, 15164–15172.

- (22) Qiu, J. X.; Petersson, E. J.; Matthews, E. E.; Schepartz, A. *J. Am. Chem. Soc.* **2006**, *128*, 11338–11339.

Peptoids provide an attractive platform to generate cyclic peptidomimetics. The submonomer chemistry protocol for peptoid synthesis allows straightforward incorporation of a large number of diverse side chain chemical functionalities.⁹ This feature, combined with the highly efficient macrocyclization reactions demonstrated in this report, provides a pathway for the discovery of peptidomimetic macrocycles exhibiting enhanced conformational ordering and diverse bioactivities. The potential for chemical modification following macrocyclization may allow peptoids to be used as conformationally defined templates upon which more complex structures can be established.

Experimental Procedures

General. Solvents and reagents purchased from commercial sources were used without further purification. Abbreviations for reagents are as follows: 9-fluorenylmethoxycarbonyl (Fmoc); *tert*-butoxycarbonyl (Boc); benzotriazole-1-yl-oxy-tris-pyrrolidinophosphonium hexafluorophosphate (PyBOP); Bromo-tris-pyrrolidinophosphonium hexafluorophosphate (PyBrOP); trifluoroacetic acid (TFA); hexafluoroisopropyl alcohol (HFIP); methylene chloride (DCM); *N,N'*-dimethylformamide (DMF); *N,N'*-diisopropylcarbodiimide (DIC); diisopropylethylamine (DIEA); acetonitrile (ACN); L-phenylalanine (Phe); *O*-methyl-L-homoserine (Hse(Me)); *N*-methylmorpholine (NMM); *O*-benzotriazole-*N,N,N',N'*-tetramethyluronium hexafluorophosphate (HBTU).

Synthesis and Purification of Peptoid Oligomers. Previously reported solid-phase peptoid synthesis protocols were used with adjustments in reaction time and washing conditions.⁹ Peptoid synthesis was performed using an automated synthesizer (Charybdis Technologies Inc., San Diego, CA) at room temperature. Peptoid oligomers were synthesized on 2-chlorotrityl chloride resin (NovaBiochem; 100–200 mesh; 1.1 mmol/g). Methoxyethylamine (Alfa Aesar) was used as a submonomer for incorporation of *N*-(methoxyethyl)glycine (*Nme*) monomer; benzylamine (Alfa Aesar) was used as a submonomer for incorporation of the *N*-(phenylmethyl)glycine (*Npm*) monomer; azidopropylamine was synthesized as previously described and used as a submonomer for incorporation of the *N*-(azidopropyl)glycine (*Naz*) residue;²³ *tert*-butyl-*N*-(3-aminopropyl)carbamate (Alfa Aesar) was used as a submonomer for incorporation of the *N*-(*tert*-butylpropylcarbamate)glycine (*Npc*) monomer; *tert*-butyl ester acetate (NovaBiochem) was used as a submonomer for incorporation of the *N*-(*tert*-butylpropionate)-glycine (*Ntp*) monomer, and *N*-*tert*-butoxycarbonylbutyldiamine was synthesized as previously described and used as a submonomer for incorporation of the *N*-(*tert*-butylbutylcarbamate)glycine (*Nab*) residue.²³ Typically, 200 mg of 2-chlorotrityl chloride resin were washed twice in 2 mL of DCM, followed by swelling in 2 mL of DCM. The first monomer was added manually by reacting 37 mg of bromoacetic acid (0.27 mmol; Sigma-Aldrich) and 189 μ L of DIEA (1.08 mmol; Chem Impex International) in 2 mL of DCM on a shaker platform for 30 min at room temperature, followed by extensive washes with DCM (five times with 2 mL) and DMF (five times with 2 mL). Bromoacylated resin was incubated with 2 mL of 1 M amine submonomer in DMF on a shaker platform for 30 min at room temperature, followed by extensive washes with DMF (five times with 2 mL). After initial manual loading of bromoacetic acid, the first submonomer displacement step and all subsequent bromoacetylation and amine displacement steps were performed by a robotic synthesizer until the desired oligomer length was obtained. The automated bromoacetylation step was performed by adding 1660 μ L of 1.2 M bromoacetic acid in DMF and 400 μ L of DIC (Chem Impex International). The mixture was agitated for 20 min, drained, and washed with DMF (three times with 2 mL). Next, 2 mL

of a 1 M solution of submonomer (2 mmol) in DMF was added to introduce the side chain by nucleophilic displacement of bromide. The mixture was agitated for 20 min, drained, washed with DMF (three times with 2 mL), and washed with DCM (three times with 2 mL). The peptoid-resin was cleaved in 2 mL of 20% HFIP (Alfa Aesar) in DCM (v/v) at room temperature. The cleavage was conducted in a glass tube with constant agitation for 30 min. HFIP/DCM was evaporated under a stream of nitrogen gas. The final product was dissolved in 5 mL of 50% ACN in HPLC grade H₂O and filtered with a 0.5 μ m stainless steel fritted syringe tip filter (Upchurch Scientific). Peptoid oligomers were analyzed on a C₁₈ reversed-phase analytical RP-HPLC column at room temperature (Peeke Scientific, 5 μ m, 120 Å , 2.0 mm \times 50 mm) using a Beckman Coulter System Gold instrument. A linear gradient of 5–95% acetonitrile/water (0.1% TFA, Acros Organics) over 20 min was used with a flow rate of 0.7 mL/min (Figure 1; analytical HPLC for **1**). Preparative HPLC was performed on a Delta-Pak C₁₈ (Waters, 15 μ m, 100 Å , 25 mm \times 100 mm) with a linear gradient of 5–95% acetonitrile/water (0.1% TFA) over 60 min with a flow rate of 5 mL/min. LC–MS was performed on an Agilent 1100 Series LC/MSD Trap XCT (Agilent Technologies). NMR data were collected with an Avance-400 NMR spectrometer (Bruker).

Synthesis and Purification of **23.** Linear peptide sequence was synthesized using standard Fmoc solid-phase peptide synthesis protocols. 200 mg of 2-chlorotrityl chloride resin (NovaBiochem; 100–200 mesh; 1.1 mmol/g) was washed twice in 2 mL of DCM, followed by swelling in 2 mL of DCM. The first amino acid was added manually by reacting 0.27 mmol of Fmoc-Phe (NovaBiochem) and 142 μ L of DIEA in 2 mL of DCM on a shaker platform for 30 min at room temperature, followed by extensive washes with DCM (five times with 2 mL) and DMF (five times with 2 mL). Resin loaded with Fmoc-Phe was incubated twice with 2 mL of 20% piperidine/DMF (v/v) on a shaker platform for 15 min at room temperature, followed by extensive washes with DMF (five times with 2 mL). After manual loading of Phe, all subsequent amino acid addition and Fmoc deprotection steps were performed on a robotic synthesizer (Charybdis Technologies Inc., San Diego, CA) until the desired peptide length was obtained. Fmoc-Hse(Me) was purchased from Senn Chemicals (Dielsdorf, Switzerland). The automated amino acid addition step was performed by adding 1 mL of 0.5 M Fmoc-amino acid in DMF, 1 mL of 0.5 M HBTU (NovaBiochem) in DMF, and 1 mL of 1.5 M NMM (Alfa Aesar) in DMF. The mixture was agitated for 30 min, drained, and washed with DMF (three times with 2 mL). Next, the resin was incubated twice with 2 mL of a 20% piperidine/DMF (v/v) for 15 min. The reaction was drained and washed with DMF (three times with 2 mL) and washed with DCM (three times with 2 mL). The peptide-resin was cleaved in 2 mL of 20% HFIP in DCM (v/v) at room temperature. The cleavage was conducted in a glass tube with constant agitation for 30 min. HFIP/DCM was evaporated under a stream of nitrogen gas. The final product was dissolved in 5 mL of 70% ACN in HPLC grade H₂O. Peptide oligomers were analyzed by RP-HPLC and ESI mass spectrometry as described above.

General Cyclization Reaction. Typical cyclization reactions were conducted in dry, deoxygenated DMF. 12 μ mol of the purified linear oligomer were suspended in 5.25 mL of DMF in a 15 mL conical tube. 375 μ L of PyBOP (NovaBiochem) solution (96 mM, freshly prepared in DMF) and 375 μ L of DIEA solution (192 mM, freshly prepared in DMF) were added to the peptoid. The reaction vessel was flushed with nitrogen and sealed to exclude air. The reaction proceeded for 5 min at room temperature, and 10 μ L of reaction mixture were diluted with 140 μ L of 50% ACN in H₂O to quench the reaction. The diluted sample was analyzed by HPLC.

Crystallization of **2.** 10 mg (13 μ mol) of **2** were dissolved in 700 μ L of HPLC grade methanol. The peptoid solution was filtered with a 0.5 μ m stainless steel fritted syringe tip filter (Upchurch Scientific). The resulting solution was subjected to slow evaporation at room

(23) (a) Pons, J. F.; Fauchere, J. L.; Lamaty, F.; Molla, A.; Lazaro, R. *Eur. J. Org. Chem.* **1998**, 853–859. (b) Carboni, B.; Benalil, A.; Vaultier, M. J. *Org. Chem.* **1993**, 58, 3736–3741.

temperature. Crystallography data: Colorless needle-like crystal, $0.05 \times 0.11 \times 0.26 \text{ mm}^3$, triclinic, $P\bar{1}$, $a = 9.307(2) \text{ \AA}$, $b = 10.423(2) \text{ \AA}$, $c = 21.794(4) \text{ \AA}$, $\alpha = 84.92(3)^\circ$, $\beta = 78.75(3)^\circ$, $\gamma = 79.41(3)^\circ$, $Z = 2$, $V = 2035.2(7) \text{ \AA}^3$, $\rho_{\text{calcd}} = 1.336 \text{ g/cm}^3$.

Crystallization of 11. 10 mg (10 μmol) of **11** were dissolved in 700 μL of HPLC grade ethanol. The peptoid solution was filtered with a 0.5 μm stainless steel fritted syringe tip filter (Upchurch Scientific). The resulting solution was subjected to slow evaporation at room temperature. Crystallography data: Colorless blocklike crystal, $0.06 \times 0.24 \times 0.40 \text{ mm}^3$, triclinic, $P\bar{1}$, $a = 15.587(3) \text{ \AA}$, $b = 18.811(4) \text{ \AA}$, $c = 20.237(4) \text{ \AA}$, $\alpha = 91.76(3)^\circ$, $\beta = 101.95(3)^\circ$, $\gamma = 106.63(3)^\circ$, $Z = 4$, $V = 5536.7(2) \text{ \AA}^3$, $\rho_{\text{calcd}} = 1.259 \text{ g/cm}^3$.

Acknowledgment. We thank Dr. Chin Lin for helpful discussions. This work was supported by the NYSTAR's James D. Watson Investigator Program. We thank the NCCR/NIH for a Research Facilities Improvement Grant (C06 RR-16572) at NYU and a Research Centers in Minority Institutions award (RR-03037) at Hunter College.

Supporting Information Available: X-ray crystallography information, RP-HPLC data, NMR spectra, mass spectrometry data, and complete refs 8b and 20c. This material is available free of charge via the Internet at <http://pubs.acs.org>.

JA066960O